Available online at www.sciencedirect.com
ScienceDirect
C. R. Chimie 12 (2009) 321–331
COMPTES RENDUS CHIMIE
http://france.elsevier.com/direct/CRAS2C/

Account / Revue

Wire-like diruthenium σ-alkynyl compounds and charge mobility therein

Bin Xi, Tong Ren*

Department of Chemistry, Purdue University, West Lafayette, IN 47907, USA

Received 8 July 2008; accepted after revision 8 September 2008
Available online 28 November 2008

Abstract

Described in this short review is the chemistry of wire-like diruthenium σ-alkynyl species, which are promising building blocks for organometallic molecular wires. Two series of carbon-rich compounds have been studied: (a) polyyn-diyls with diruthenium capping units, and (b) bi-ferrocenes with a diruthenium alkynyl bridge. Investigations of both the charge transfer process across the polyyn-diyls and the role of diruthenium cores in enhancing charge mobility are achieved through X-ray structure determination, spectroscopic, voltammetric and spectroelectrochemical measurements. ***To cite this article: B. Xi, T. Ren, C. R. Chimie 12 (2009).***

Keywords: Diruthenium; Polyyn-diyl bridge; Molecular wire; Alkynyl organometallics

1. Introduction

The study of transition-metal σ-alkynyl complexes can be traced back to 1960s [1,2]. Since the mid-1980s, this area has attracted much more intense interests as evidenced by increasing numbers of research papers from approximately 200 to over 20,000 [3]. Compared with the pure organic conjugated systems [4,5], introduction of metal units into the polymeric or oligomeric systems may result in a broad range of improved properties including electronic communication (molecular wires) [6,7], nonlinear optical effects [8], luminescence and photoconductivity [9,10].

In the research of utilizing metal σ-alkynyl complexes as building blocks for molecular electronic devices, two types of metal alkynyl wires were proposed (Chart 1) [6,11]. Polyyn-diyls (C_{2n}) capped by two metal termini (type **I** in Chart 1) are very attractive prototypes of ''organometallic molecular wires''. Many of the pioneering efforts focused on the design of type **I** wires featuring facile charge transfer across the *sp* carbon chain (polyyn-diyls), with [M] as CpFe(P–P) [12], CpRe(P)NO [13–15], $CpRu(P)_2$ [16], and $Mn(P–P)_2I$ [17] where P and P–P denote mono- and bidentate phosphines, respectively. Monodisperse oligomers (type **II** in Chart 1) could be better alternatives than dimers (**I**) on the aspects of controlling length and connecting to the outside world, from the practical applications point of view. However, some limitations preclude the possibility of many metal complexes as candidates for type **II** wires. To form oligomers, the metal units should be capable of forming bis-alkynyl complexes, and in addition, the selection of the metal center [M] is also critical to avoid insulating behavior [6,18]. Examples of

* Corresponding author.
E-mail address: tren@purdue.edu (T. Ren).

1631-0748/$ - see front matter
doi:10.1016/j.crci.2008.09.017

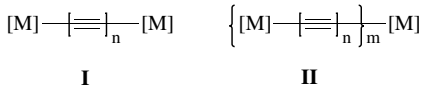

I **II**

Chart 1. Dimeric (**I**) and metallayne (**II**) wires.

well-characterized type **II** oligomers are rare, and those based on $Ru_2(DPhF)_4$-butadiynyl [19] and $Ru(P{-}P)_2{-}\sigma$-arylacetylide monomers [20,21] are noteworthy.

Our effort in developing organometallic molecular wires focuses on using diruthenium paddlewheel species as [M] [22–25], due to their attractive features including the controlled syntheses of the mono- and bis-alkynyl complexes, the stability toward ambient atmosphere and heat, the redox flexibility, and very small HOMO–LUMO gaps (1.2–1.5 eV) [26–34]. As excellent chromophores and electrophores, the diruthenium alkynyl complexes have been studied as promising building blocks for novel (opto)electronic materials [23].

2. Ru_2 polyyn-diyls

Our investigation of diruthenium alkynyl compounds of a paddlewheel motif demonstrated that σ-alkynyl compounds of $[Ru_2L_4]$ have good charge mobility along the axial direction. Ru_2(II,III) based wire-like compounds (type **I**) with n up to 10 have been prepared with various supporting ligands (L). Compounds of long polyyn-diyl segments are desired for better understanding of the electron coupling within the type **I** molecules and the distance dependence of H_{ad} (adiabatic electronic coupling elements).

The *N*,*N*′-bidentate bridging ligands (L) utilized in supporting the Ru_2 core include 2-anilinopyridinate (*ap*) and its anilino-substituted derivatives, 2-(3,5-dimethoxyanilino)pyridinate (DiMeO*ap*), and 2-(*i*-butoxyanilino)pyridinate (*i*BuO*ap*) (Chart 2). Using *ap* as the auxiliary ligand, type **I** compounds with *n* up to 6 were prepared and studied [35,36]. Both of the modified *ap* ligands afford significantly improved solubility in common organic solvents [37,38], and

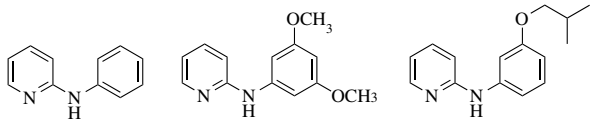

ap **H-DiMeO*ap*** **H-iBuO*ap***

Chart 2. *N*,*N*′-bidentate ligands supporting the Ru_2 core.

facilitate the preparation of type **I** compounds with *n* up to 10, and the access to compounds of odd *n* as well.

2.1. Monomers and dimers

Wire-like molecules $[Ru_2L_4]_2(\mu\text{-}C_2)$, $[Ru_2L_4]_2(\mu\text{-}C_4)$ and $[Ru_2L_4]_2(\mu\text{-}C_6)$ (L = DiMeO*ap*, compounds **A1**–**A3**; L = *ap*, compounds **A1′**–**A3′**) were synthesized through anion metathesis between $[Ru_2L_4]{-}Cl$ and $LiC_{2n}Li$ [35,36]. However, this technique became impractical with longer polyyn-diyl ligands, due to the instability of $LiC_{2n}Li$ with $n \geq 4$. Hence, the longer type **I** compounds ($n \geq 4$) were prepared through the Glaser oxidative coupling [39] of their corresponding "half" molecules which are the monomer type in Chart 3.

The mono-adduct with $k = 2$ was prepared from a reaction between $[Ru_2L_4]{-}Cl$ and LiC_4SiMe_3. After the removal of terminal protection group $-SiMe_3$ (K_2CO_3, THF/MeOH), a two-carbon sp chain extension reaction was achieved by the Glaser oxidative coupling [39] of $[Ru_2L_4]{-}C_4H$ and excess $HC{\equiv}CSiMe_3$ (*Hay* conditions: O_2, cat. CuCl, TMEDA and acetone) to give $[Ru_2L_4]{-}C_6SiMe_3$ (monomer with $k = 3$). However, extending this sequence to longer monomers ($k = 4$ and 5) was unsuccessful with the problem of increasing tendency for homo-coupling of $[Ru_2L_4]{-}C_{2k}H$ during the reaction. The *Cadiot–Chodkiewicz* (Cadiot for short) coupling method [39] was successfully employed by Gladysz and coworkers to extend $Re{-}(C{\equiv}C)_n{-}$ chains [40], which involved the formation of a copper alkynyl complex intermediate. As shown in Scheme 1, the extension of $Ru_2{-}(C{\equiv}C)_k{-}$ monomers ($k > 2$) under *Cadiot* conditions was achieved with significantly

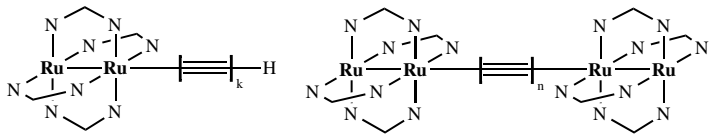

$[Ru_2L_4](C_{2k}H)$ mono-adduct **$[Ru_2L_4](\mu\text{–}C_{2n})[Ru_2L_4]$** bridge complex

Chart 3. Diruthenium mono-alkynyl building block and wire-like bridge compound.

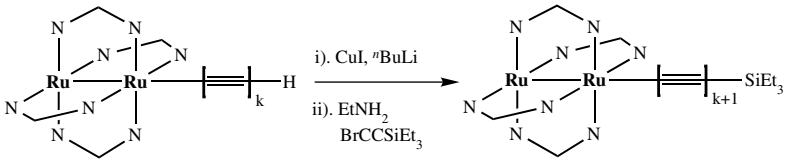

Scheme 1. Extension of carbon chain for monomers through Cadiot coupling.

increased yields compared to those under *Hay* conditions.

The longer dimers, namely the $[Ru_2L_4](\mu\text{-}C_{2n})[Ru_2L_4]$ ($n \geq 4$) type compounds (Chart 3), were synthesized through either oxidative homo-coupling of corresponding monomers (for dimers with even-numbered n (C_8, C_{12}, C_{16} and C_{20})) or cross coupling of two different monomers (for type **I** dimers with odd n (C_{10}, C_{14} and C_{18})) (Scheme 2), under *Hay* conditions in moderate to good yields. During the preparation of the latter type compounds, symmetric dimers ($Ru_2{-}\mu\text{-}C_{2n}{-}Ru_2$ and $Ru_2'{-}\mu\text{-}C_{2n}{-}Ru_2'$) were generated as the byproducts and tedious chromatography, typically preparative TLC, was necessitated for separation.

Type **I** dimers are generally difficult to crystallize and only molecules containing C_4 (short), C_6 (short), and C_8 (medium) bridges have been structurally characterized in our diruthenium system (Fig. 1) [23,35,36].

Clearly, the coordination environment of the $[Ru_2L_4]$ cores in dimers is identical to that of monomer type compounds (i.e. $[Ru_2L_4]{-}C_2Y$). The *N*,*N*′-bidentate bridging ligands in both monomers and dimers adopt the (4,0) arrangement, namely that all anilino N-centers coordinate to the Ru center (4 site) and all pyridine N-centers coordinate to the other Ru center (0 site). Compared to its corresponding monomer, there is no significant change of Ru–Ru distance in the dimer (~2.33 Å), while Ru–C_α bond became shorter (~2.02 Å) due to the strengthened Ru–C_α interaction on the formation of polyyn-diyls systems.

2.2. Characterizations

2.2.1. Redox properties

In the type **I** compounds, exploration of the electron mobility across the polyyn-diyl chains is related to the investigation of the electronic coupling between two redox-active $[Ru_2L_4]$ moieties, which was assessed on the basis of the comparison of their voltammetric behavior (CV/DPV) with that of the ''half'' molecule (monomer). For instance, the cyclic voltammogram of monomer $[Ru_2]{-}C_4TMS$ ($[Ru_2] = [Ru_2(DiMeOap)_4]$) exhibits two reversible one-electron processes at ca. 0.5 V (oxidation) and ca. −0.7 V (reduction) [38]. On the other hand, the dimer molecule, $[Ru_2]_2(\mu\text{-}C_6)$ (**A3**) clearly exhibits more complex redox features including multiple reversible one-electron couples within the same potential window (Fig. 2): two stepwise oxidations (2+/1+) and (+1/0) at potentials close to 0.5 V and two stepwise reductions (0/−1) and (−1/−2) at potentials close to −0.7 V. Both oxidation couples and the first (least cathodic) two reduction couples are Ru_2 based. The pairwise appearance of one-electron couples instead of a two-electron wave is an indicative of significant electronic coupling between two $[Ru_2]$ units. Moreover, the potential splitting within each pair ($\Delta E_{1/2}$) is proportional to the coupling strength and can serve as a *qualitative* indictor, as well known in the mixed-valence chemistry [41–43]. In addition, the potential differences within the oxidations ($\Delta E_{1/2}(+1)$) and reductions ($\Delta E_{1/2}(-1)$) allow the estimation of comproportionation constants for the corresponding mixed-valence cation ($K_{com}(+1)$)and anion ($K_{com}(-1)$), respectively [41–44],

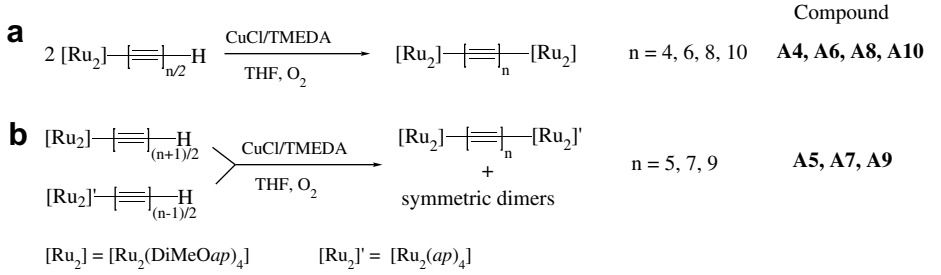

Scheme 2. Homo/cross-coupling of mono-adduct to yield dimers.

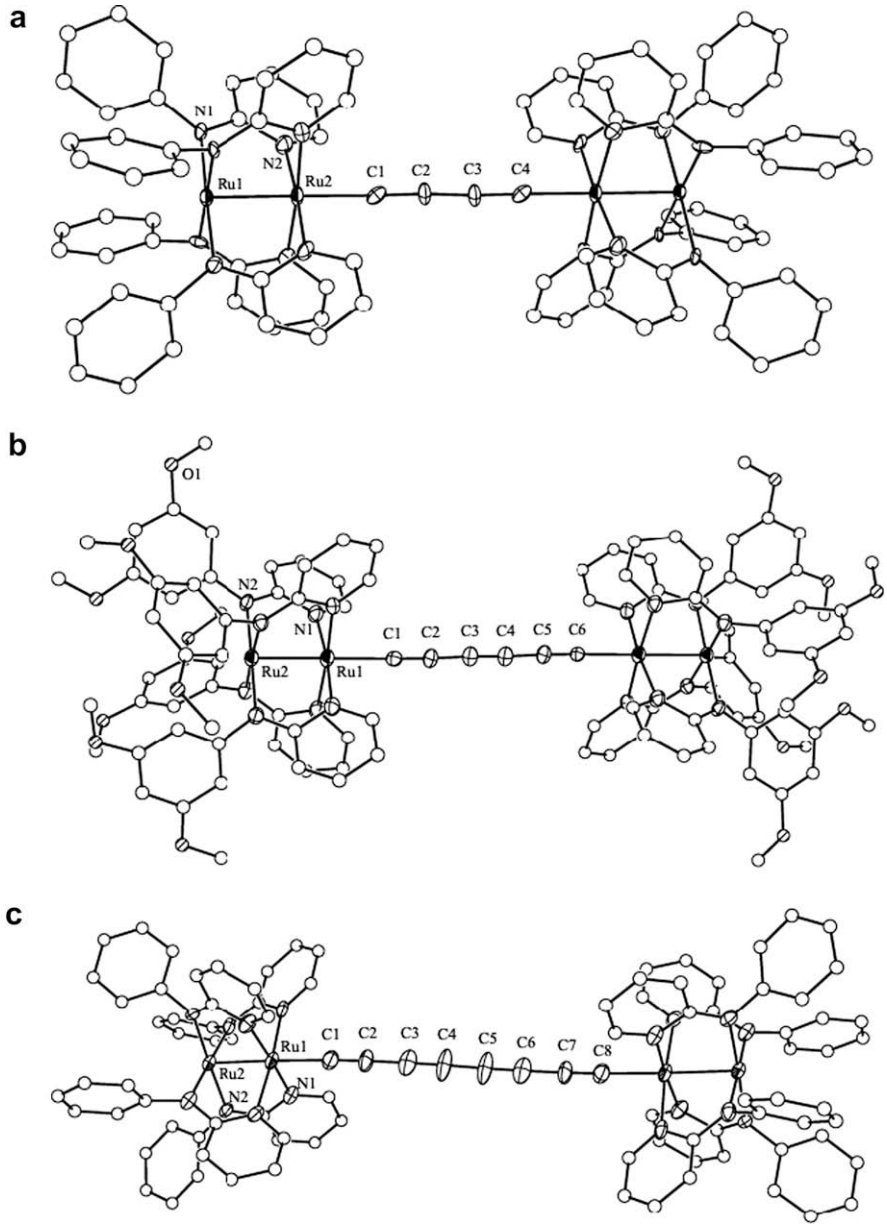

Fig. 1. Structural plots of (a) $[Ru_2(ap)_4]_2(\mu\text{-}C_4)$, (b) $[Ru_2(DiMeOap)_4]_2(\mu\text{-}C_6)$, (c) $[Ru_2(ap)_4]_2(\mu\text{-}C_8)$.

which are summarized in Table 1. Finally, $[Ru_2L_4]$ monomers with L as both *ap* and DiMeO*ap* exhibit almost identical redox potentials (differences within 30 mV), which indicates minimal effect of ligand L on the electronic structures of Ru_2 core [38,45].

The voltammetric plots (differential pulse voltammetry) in Fig. 3 and electrode potential data in Table 1 reveal similar redox behaviors within $[Ru_2L_4]_2(\mu\text{-}C_{2n})$ type compounds and some noteworthy trends. First, for each dimer, the difference between $E_{1/2}(0/-1)$ and $E_{1/2}(-1/-2)$ ($\Delta E_{1/2}(-1)$) is much larger than the difference between $E_{1/2}(+2/+1)$ and $E_{1/2}(+1/0)$ ($\Delta E_{1/2}(+1)$), which suggests that the $[Ru_2L_4]_2(\mu\text{-}C_{2n})$ type compounds are much better electron carrier than hole carrier, partly due to the electron-deficient nature of both the diruthenium core and polyyn-diyl bridge [36]. Second, as the polyyn-diyl chain elongates, both $\Delta E_{1/2}(+1)$ and $\Delta E_{1/2}(-1)$ gradually decrease (from resolved one-electron couples to merged pseudo two-electron waves) indicating the decrease of electronic coupling

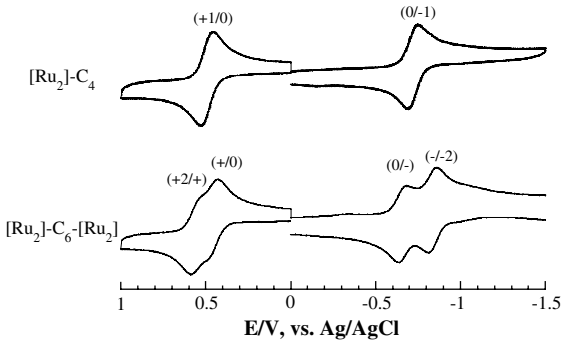

Fig. 2. Cyclic voltammograms of $[Ru_2]-C_4TMS$ (monomer) and **A3** (dimer) recorded in 0.20 M THF solution of Bu_4NPF_6 at a scan rate of 0.10 V/s.

between two Ru_2 centers. This trend is consistent with the consensus that the degree of coupling between a pair of donor–acceptor centers decays exponentially as the distance increases [41,43,46]. Third, potentials for all redox couples display a significant anodic shift as the polyyne chain elongates, which is attributed to the electron-deficient nature of the added acetylene units. Additionally, the second pair of one-electron reductions at more negative potentials was tentatively assigned as polyyn-diyl based [36].

2.2.2. Spectroelectrochemistry

As established in the mixed-valence chemistry, the splitting in potentials of oxidation/reduction pairs ($\Delta E_{1/2}$) and the resultant comproportionation constant K_{com} usually serve as *qualitative* indicators of the nature of mixed-valency. These parameters generated from the electrochemical measurements significantly depend on the nature of solvents and electrolytes [47], and hence may be inappropriate as *quantitative* measures. A more suitable approach is to examine spectroscopic characteristics of the mixed-valence species, namely the intervalence transitions between donor and acceptor Ru_2 moieties as mediated by the polyyn-diyl bridge, through spectroelectrochemical studies [41,43,44,48]. Fig. 4 shows electronic absorption spectra derived from spectroelectrochemical studies of $[Ru_2(ap)_4]_2(\mu\text{-}C_4)$ **A2′** and its reference compound $Ru_2(ap)_4(C_2TMS)$ [36]. Upon either one-electron reduction or one-electron oxidation, intervalence charge transfer (IVCT) bands appeared and half-widths (bandwidths at half-peak height) were estimated from spectral deconvolution assuming Gaussian profiles (data are summarized in Table 2). The band at ca. 8450 cm^{-1} is clearly attributed to the CT between two Ru_2 moieties of $\{[Ru_2(ap)_4]_2(\mu\text{-}C_4)\}^{-1}$. The lower energy band (5670 cm^{-1}) is likely due to the mixing of LMCT and IVCT states in such

Table 1
Electrode potentials (V) for dimers **A3**–**A9** from DPV measurement[a]

Compounds	+2/+1	+1/0	0/−1	−1/−2	−2/−3	−3/−4	$K_{com}(-1)$[b]
A3	0.54	0.44	−0.65	−0.83	−1.81	−2.80	1300
A4	0.54 (2e⁻)		−0.57	−0.72	−1.68	−1.94	370
A5	0.56 (2e⁻)		−0.52	−0.64	−1.55	−1.80	130
A6	0.57 (2e⁻)		−0.45	−0.57	−1.42	−1.69	110
A7	0.58 (2e⁻)		−0.43	−0.54	−1.31	−1.60	70
A8	0.58 (2e⁻)		−0.39	−0.49	−1.19	−1.51	60
A9	0.59 (2e⁻)		−0.36	−0.45	−1.07	−1.43	40

[a] Unpublished results.
[b] $K_{com}(-1) = \exp(\Delta E_{1/2}/0.0257)$ at 25 °C.

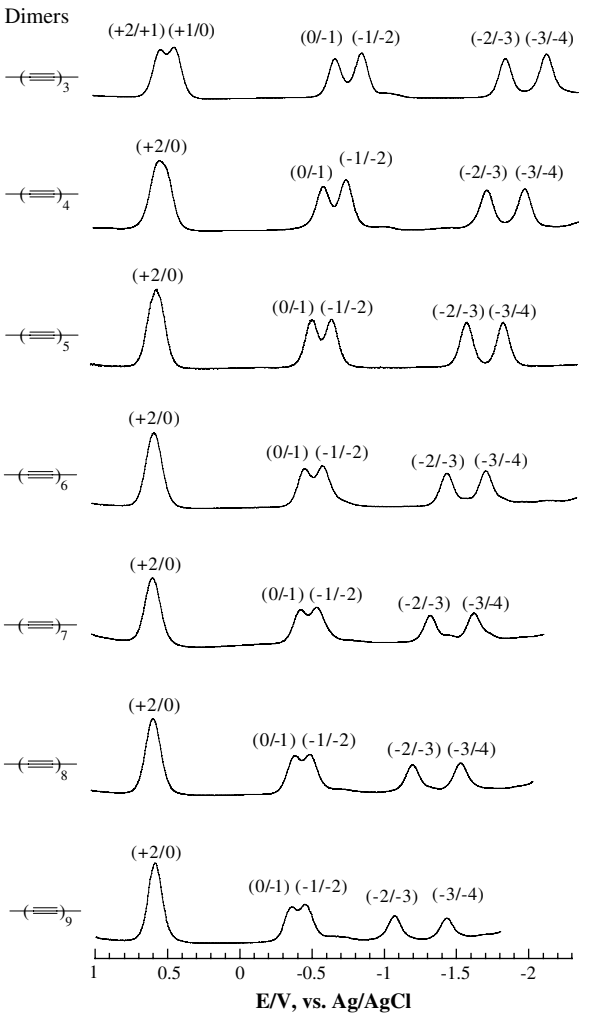

Fig. 3. Differential pulse voltammograms of dimers **A3**–**A9** recorded in 0.20 M THF solution of Bu_4NPF_6 at a scan rate of 0.10 V/s.

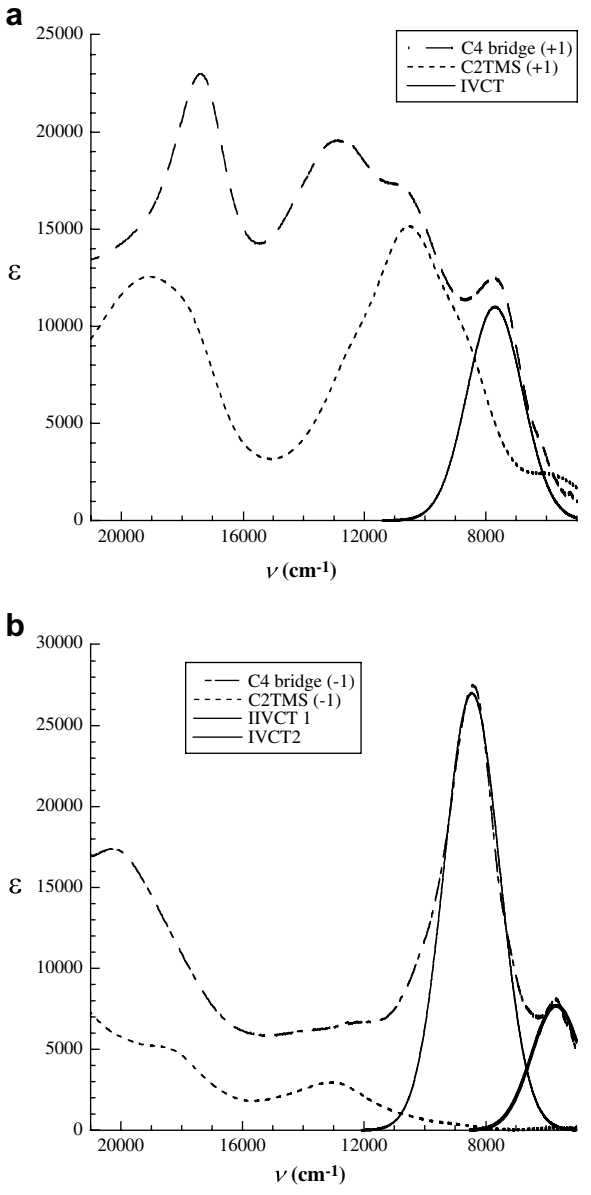

Fig. 4. Spectroelectrochemistry results of **A2′** and its "half" molecule $Ru_2(ap)_4(C_2TMS)$: (a) spectra with one deconvoluted IVCT band upon one-electron oxidation (b) spectra with two deconvoluted IVCT bands upon one-electron reduction.

a strongly delocalized system, and a definitive answer awaits a high level computational study. Based on the comparison of the estimated half-widths with those predicted from the Hush model, which describes weakly coupled mixed-valence species (Robin-Day class II) [49,50], the mixed-valence cation and anion of compound **A2′** are strongly coupled species due to the narrowness of the observed IVCT bands [36,44]. They may be regarded as the class III species close to the borderline of class II–III using the Γ parameter analysis [51].

Table 2
Spectroelectrochemistry results[a] of mixed-valence ions of $[Ru_2(ap)_4]_2(\mu\text{-}C_4)$.

Mixed-valence species	E_{IVCT}	ε	$\Delta\nu_{1/2}$	$\Delta\nu_{1/2}$(Hush)[b]	Γ[c]
$(\mathbf{A2}')^{1-}$	8450	27000	1820	4420	0.59
	5670	7700	1630	3620	0.55
$(\mathbf{A2}')^{1+}$	7700	11000	1820	4220	0.57

[a] E_{IVCT}, $\Delta\nu_{1/2}$ and $\Delta\nu_{1/2}$(Hush) in cm^{-1} and extinction coefficient (ε) in $M^{-1}\,cm^{-1}$.
[b] $\Delta\nu_{1/2}(\text{Hush}) = (2310\nu_{max})^{1/2}$.
[c] $\Gamma = 1 - \Delta\nu_{1/2}/\Delta\nu_{1/2}(\text{Hush})$.

The IVCT bands are also useful in estimating the adiabatic electronic coupling element H_{ad} for the series of $[Ru_2L_4]_2(\mu\text{-}C_{2n})$ through $H_{ad} = (\Delta G_r E_{IVCT})^{1/2}$, where ΔG_r is the free energy of resonance exchange and E_{IVCT} is related to the energy of IVCT band [52]. Furthermore, the electronic coupling attenuation constant γ, an efficient measure of the medium's ability to mediate electronic coupling, can be extracted using the equation $H_{ad} = H_0 \exp(-\gamma R)$, where H_{ad} and H_0 are donor and acceptor wave function resonance exchanges at distance R and van der Waals contact distance, respectively, and R is the separation between the donor and acceptor from van der Waals contacts [41,43,44]. The success of extending the polyyn-diyl bridge to C_{20} provides the possibility of probing the electronic coupling over a long distance. For the reduced mixed-valence ions of the $[Ru_2L_4]_2(\mu\text{-}C_{2n})$ compounds, two estimated γ were derived from a $\ln(H_{ad})$ versus $d_{Ru_2-Ru_2}$ plot[1] (Fig. 5): $\gamma_1 = 0.100$ Å^{-1} for $n = 1$–3 and $\gamma_2 = 0.015$ Å^{-1} for $n = 4$–10, which are comparable to that found for oligoene-bridged pentaammineruthenium(II,III) donor–acceptor pairs ($\gamma = 0.070$ Å^{-1}) [53] and Fc–Fc$^+$ donor–acceptor pairs ($\gamma = 0.087$ Å^{-1}) [54]. The appearance of dual attenuation parameters (bimodal) within a homologous series of molecules is relative rare [55], but has been frequently documented in electron transfer mediated by peptide chains [56]. The bimodal behavior in the latter case has been interpreted as superexchange (tunneling) at shorter distances and hopping at longer distances, although the precise mechanisms await more detailed studies.

[1] The energies of IVCT for most of the members in this series are currently unavailable and that of **A2′** was used instead.

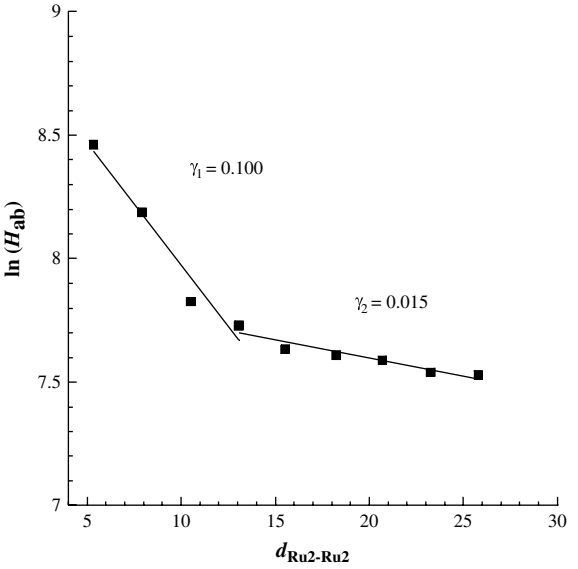

Fig. 5. Distance-dependence plot of $\ln(H_{ad})$ (H_{ad} in cm^{-1}) versus $d_{Ru_2-Ru_2}$ (in Å).

3. Ru_2 bis-alkynyls capped by Fc termini

To realize the molecular wire as proposed in Chart 1, not only the charge transfer process on linear conjugated polyyn-diyl chains should be investigated, but also the role of the Ru_2 core in mediating electron mobility needs to be addressed [57,58]. This is realized by covalently attaching a pair of ferrocenyl units at the opposite ends of the Ru_2 fragment [Fc(C≡C)$_n$–Ru_2–(C≡C)$_m$Fc] and using both the comproportionation constant $K_{com} = \exp(\Delta E_c/0.0257)$ (at room temperature, and ΔE_c is defined by the equation below) [59] and spectroscopic characteristics of the mixed-valence ions to study the electron delocalization across the Ru_2 core [49].

$$\text{Fc-[Ru}_2\text{]-Fc} \underset{E_{1/2}(\text{II})}{\overset{-\,e^-}{\rightleftharpoons}} \text{Fc-[Ru}_2\text{]-Fc}^+ \underset{E_{1/2}(\text{I})}{\overset{-\,e^-}{\rightleftharpoons}} \text{Fc}^+\text{-[Ru}_2\text{]-Fc}^+$$

$$\Delta E_c = E_{1/2}(\text{II}) - E_{1/2}(\text{I})$$

In this diruthenium bis-alkynyl series, the *N*,*N*′-bidentate bridging ligands (L) utilized in supporting the Ru_2 core are *N*,*N*′-dimethylbenzamidinate (DMBA) and its phenyl-substituted derivative, *N*,*N*′-dimethyl-3-methoxy-benzamidinate (MeODMBA) (Chart 4). The modified DMBA ligand also has the advantage of significantly improved solubility of bis-compounds in common organic solvents [60].

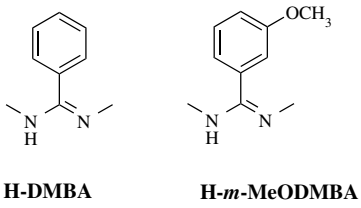

H-DMBA **H-*m*-MeODMBA**

Chart 4. *N*,*N*′-dimethylbenzamidinate and its modified ligand.

3.1. Alkynylation protocols

A series of diruthenium bis-alkynyl compounds which contain two Fc termini *trans*-(FcC$_{2n}$)[Ru_2(Y-DMBA)4](C$_{2m}$Fc) (Chart 5) were successfully synthesized through either anion metathesis [57,58] route or the weak-base protocol (Scheme 3) [23,60–63].

Weak-base protocol is superior to anion metathesis for the preparation of compounds containing functional groups (i.e. $-NO_2$, $-CN$) sensitive to organolithium agents [61]. In addition, anaerobic or anhydrous conditions are not required, which facilitates the reaction monitoring and optimization (choice of base and stoichiometry of reactions) [23,63].

Symmetric compounds [Ru_2(Y-DMBA)4](C$_{2n}$Fc)$_2$ were prepared in excellent yields, while unsymmetric compounds (FcC$_{2n}$)[Ru_2(Y-DMBA)4](C$_{2m}$Fc) were produced at lower yields after chromatographic separation from the symmetric compounds [57,58]. It is notable that compounds [Ru_2(Y-DMBA)4](C$_6$Fc)$_2$ and [Ru_2(Y-DMBA)4](C$_8$Fc)$_2$ cannot be synthesized through reactions between Ru_2(Y-DMBA)$_4$Cl$_2$ and Li(C≡C)$_n$Fc ($n = 3$ and 4), due to the instability and difficult isolation of H(C≡C)$_n$Fc ($n \geq 3$) [64].

Crystallization of the series of bis-alkynyl compounds was successful on less soluble Ru_2(DMBA)4-based complexes [58]. Fig. 6 shows structural plots of compounds **B1**–**B3** determined via single-crystal X-ray diffraction and reveals similar structures under successive extensions by one acetylene unit [57,58]. Other features are: (1) two ferrocenyl groups occupy the opposite axial positions, and the longest edge–edge distance between

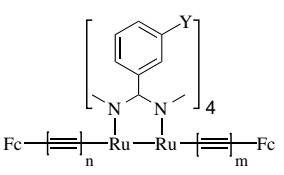

n	m	Compound Y=H, -OCH$_3$	
1	1	**B1**	**B1'**
1	2	**B2**	**B2'**
2	2	**B3**	**B3'**
3	3	**B4**	**B4'**
4	4	**B5**	**B5'**

Chart 5. *trans*-(FcC$_{2n}$)[Ru_2(Y-DMBA)4](C$_{2m}$Fc) series.

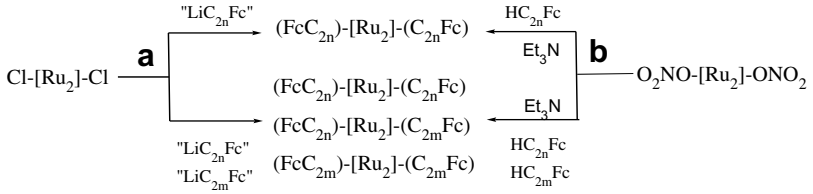

Scheme 3. Synthetic routes (a) anion metathesis (b) weak-base protocol to the Fc-capped symmetric and unsymmetric compounds ([Ru2] = "Ru2(DMBA)" or "Ru2(MeODMBA)").

two Fc centers ($C_\omega \ldots C_\omega'$) is calculated as 21.6 Å for the symmetric compound **B4**; (2) the relative orientations between two Fc units are either almost *trans* to each other in **B1** (162°) or close to orthogonal in **B2** (104°) [58]; (3) In compounds **B1** and **B2**, Ru–N bond lengths vary and Ru′–Ru–C angles deviate from linearity. Such distortions from an idealized D_{4h} geometry have been documented in many bis-alkynyl compounds of a Ru_2(III,III) core and were addressed by a second-order Jahn–Teller effect [31,32,60,61].

3.2. Characterizations

3.2.1. Redox properties

Both the cyclic and differential pulse voltammograms of more soluble Ru_2(*m*-MeODMBA)$_4$-based compounds recorded in THF are shown in Fig. 7. For instance, compound **B1′** exhibits three sequential one-electron oxidations (between +0.4 V and +1.0 V) and one one-electron reduction at ~ −1.2 V in the potential window of −1.5–+1.5 V (vs. Ag/AgCl). Spectroelectrochemical studies (details discussed below) identified the reduction and first oxidation as Ru_2 based, while the second and third oxidations as Fc based. While the butadiynyl spaced di-ferrocene (Fc(C≡C)$_4$Fc) to a pseudo two-electron oxidation [65], compound **B1′** displays a remarkably large potential splitting of 310 mV, indicating a strong coupling between two ferrocenyl units ($K_{com} \approx 173\,000$). As the Fc…Fc distance increases, similar redox behaviors to those illustrated in the [Ru_2]–(μ-C_{2n})–[Ru_2] are observed: (1) all redox couples are positively shifted, which is attributed to the strong electron-withdrawing nature of the added acetylene units; (2) Ru_2 oxidation couples drastically shift and overlap with the first Fc oxidation couples as *n* is increased to generate a two-electron wave.

3.2.2. Spectroelectrochemistry

Since the reduction couple is Ru_2 based, spectroelectrochemical measurements focused on oxidations

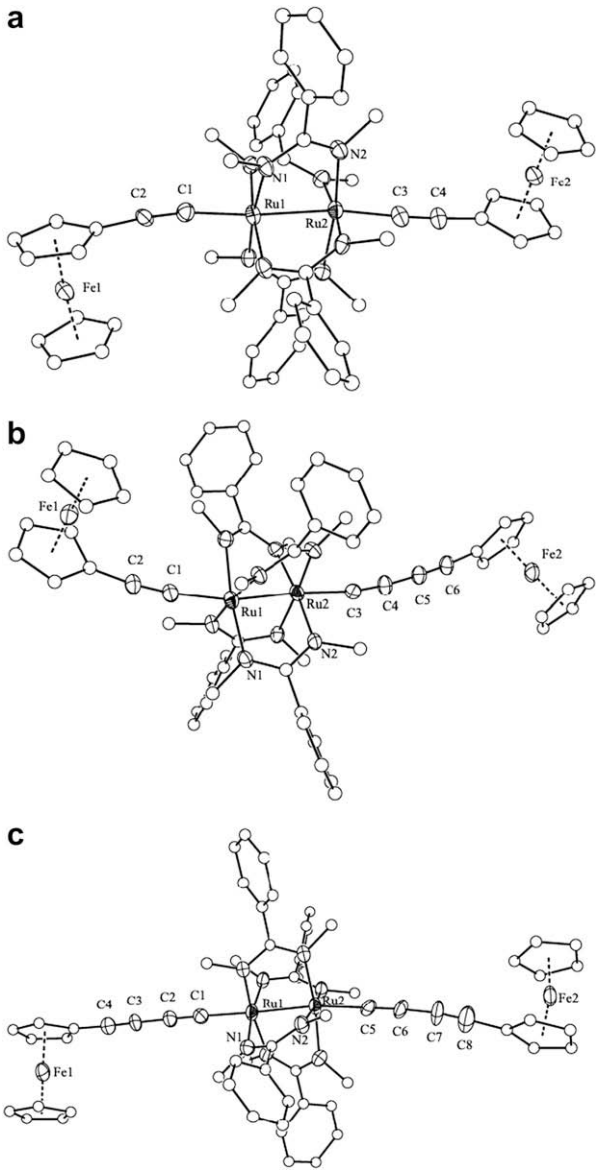

Fig. 6. Structural plots of (a) [Ru_2(DMBA)4](C$_2$Fc)$_2$ (**B1**), (b) [Ru_2(DMBA)4](C$_2$Fc)(C$_4$Fc) (**B2**), (c) [Ru_2(DMBA)4](C$_4$Fc)$_2$ (**B3**).

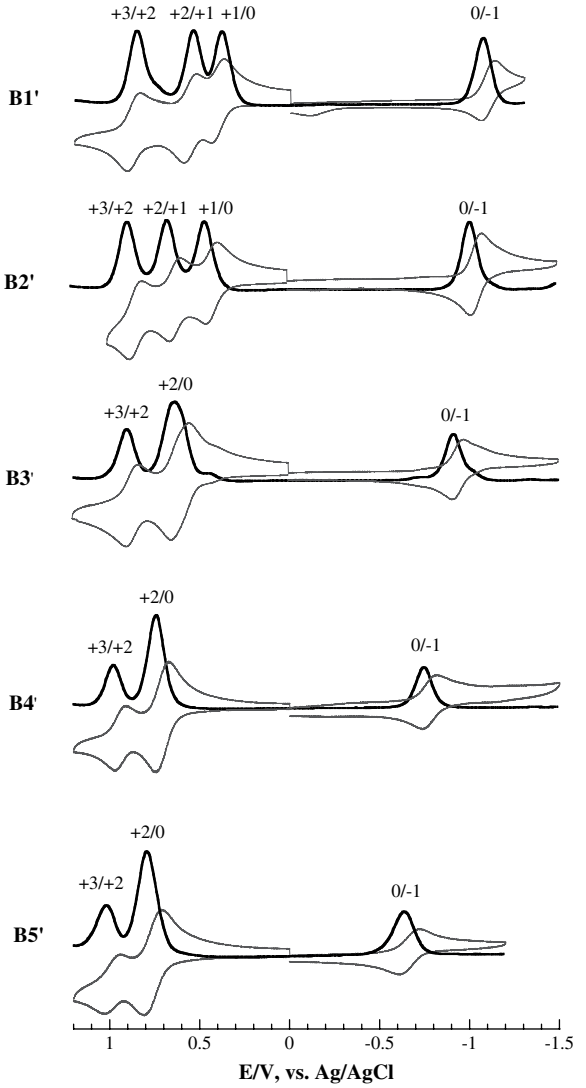

Fig. 7. Electrochemical results of *trans*-(FcC_{2n})[Ru_2(MeODMBA)4] (C_{2m}Fc) series (compounds **B1′**–**B5′**) recorded in 0.20 M THF solution of Bu_4NPF_6 at a scan rate of 0.10 V/s with a glassy carbon working electrode.

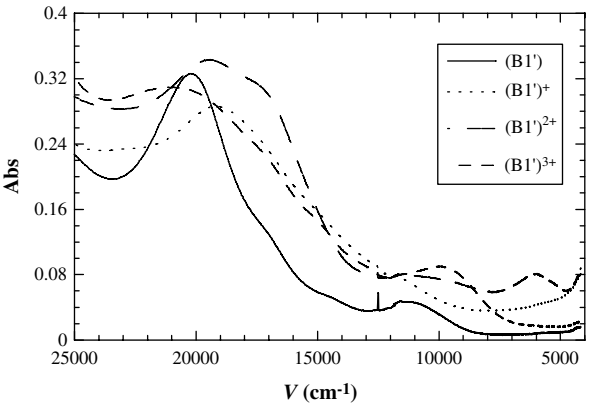

Fig. 8. Spectroelectrochemistry results of **B1′** upon sequential one-electron oxidation.

only [57,58]. Spectroelectrochemical study of symmetric compound **B1′** provided absorption spectra of its oxidation products $(\mathbf{B1'})^{+}$, $(\mathbf{B1'})^{2+}$ and $(\mathbf{B1'})^{3+}$, which show clean isosbestic points with good reversibility (>95% recovery) (Fig. 8). The first oxidation to $(\mathbf{B1'})^{+}$ resulted in appearance of a very broad low energy band (band I) in the spectrum extending from the near-IR to IR region, with the maximum absorption out of the spectral range of study. The spectrum of dication $(\mathbf{B1'})^{2+}$ displays a new higher energy band (band II) around 6000 cm^{-1} in addition to band I. Upon third oxidation to $(\mathbf{B1'})^{3+}$, both bands disappeared. Bands I and II are assigned to IVCT bands; which vanished in $(\mathbf{B1'})^{3+}$ since both Fe are in the 3+ state. Compared to the IVCT bands observed for biferrocene [65], band II has approximately the same energy and hence is assigned as Fc–$[Ru_2]^{+}$–Fc^{+} based (Fc to Fc^{+} transition). The other two oxidized forms are Fc–$[Ru_2]^{+}$–Fc ($(\mathbf{B1'})^{+}$, mixed-valent, Fc to Ru_2^{7+} transition) and Fc^{+}–$[Ru_2]^{+}$–Fc^{+} ($(\mathbf{B1'})^{3+}$, no transitions), respectively. Unsymmetrical compound **B2′** and symmetric compound **B3′** exhibit similar spectroelectrochemical behaviors and data related to their mixed-valent species are listed in Table 3. Bandwidths of Fc to Fc^{+} IVCT are generally narrower than those predicted by Hush model, even across a distance of 16.6 Å [23,49,57,58]. Obviously, the characteristics of the IVCT band are consistent with the magnitude of the comproportionation constants, indicating a valence delocalized state. The extent of delocaliztion is sufficient to classify $(\mathbf{B1'})^{2+}$, $(\mathbf{B2'})^{2+}$ and $(\mathbf{B3'})^{2+}$ as Robin-Day class **III**, class **II–III** and **II–III** species, respectively [50,51]. In contrast, other Fc–X–Fc^{+} systems (with X = none, acetylene, butadiyne or metal-containing units) exhibit very weak electronic communication despite short Fc–Fc^{+} distances [65–67]. Thus, all these results evidence the proficiency of $[Ru_2]$ core in mediating superexchange electronic coupling (especially *hole* transfer) over a long distance. The mechanism of $[Ru_2]$ acting as an efficient charge transfer bridge is under investigation.

4. Conclusions and outlook

Reviewed herein is our exploration in the chemistry of wire-like diruthenium σ-alkynyl species (Chart 1), including their syntheses, structural characterization, bulk solution voltammetry and

Table 3
Electrochemical and spectroelectrochemical results of Fc–X–Fc$^+$ type species.

Fc–X–Fc$^+$	$C_\omega \ldots C_\omega'$[a]	K_{com}	E_{IVCT}[a]	$\Delta\nu_{1/2}$	$\Delta\nu_{1/2}$(Hush)[b]	Γ	ref
None	1.45	821 000	5000	3700	3400	–	[57]
$-C_2-$	4.0	7700	6410	5000	3850	–	[56]
$-C_4-$	6.8	50	8470	5000	4420	–	[56]
$-C_2Ru(dppm)_2C_2-$	9.36	5200	4770	3300	3320	–	[58]
B1′	11.58	173 000	6000	800	3720	0.78	[50,51]
B2′	13.84	3500	6230	1520	3790	0.60	[51]
B3′	16.60	–	6680	1780	3930	0.55	[51]

[a] $C_\omega \ldots C_\omega'$ (in Å) is the edge–edge distance between two Fc centers, E_{IVCT}, $\Delta\nu_{1/2}$ and $\Delta\nu_{1/2}$(Hush) in cm^{-1}.
[b] $\Delta\nu_{1/2}(\text{Hush}) = (2310\nu_{max})^{1/2}$.

spectroelectrochemistry. Facile *electron* transfer across the polyyn-diyl chains was demonstrated and very small electronic coupling attenuation constants were determined, which favor the realization of the proposed molecule wires [68,69]. Also illustrated is the exceptional ability of diruthenium unit in enhancing charge mobility (especially *hole* mobility) on the basis of the studies of the *trans*-(FcC$_{2n}$)[Ru$_2$(Y-DMBA)4](C$_{2m}$Fc) series. Nevertheless, several pertinent issues remain unresolved: (1) charge transfer mechanisms resulting in two different attenuation constants in one system [Ru$_2$]–(μ-C$_{2n}$)–[Ru$_2$] and (2) mechanism of [Ru$_2$] acting as an efficient charge transfer bridge between two ferrocenes. Also, the access to type **I** compounds with *n* beyond 10 is a challenging task, although one may find comfort in the recent breakthrough of Gladysz in preparing diplatinum compounds of *n* up to 14 [70,71]. Other related future efforts include seeking the in-depth knowledge of the ground-state electronic structures and the spectroscopic characteristics of these carbon-rich systems, controlling the direction of charge transfer (rectification) through donor/acceptor functionalization [63], and studying the distance dependence of the spin–spin interaction between two [Ru$_2$] units [23,58].

Acknowledgement

Financial support from the National Science Foundation (CHE 0715404) and Purdue University is gratefully acknowledged.

References

[1] R. Nast, Coord. Chem. Rev. 47 (1982) 89.
[2] N. Hagihara, K. Sonogashira, S. Takahashi, Adv. Polym. Sci. 40 (1980) 149.
[3] N.J. Long, C.K. Williams, Angew. Chem. Int. Ed. 42 (2003) 2586.
[4] M.M. Haley, R.R. Tykwinski (Eds.), Carbon-rich Compounds: From Molecules to Materials, Wiley-VCH, Weinheim, 2006.
[5] F. Diederich, R.R. Tykwinski, P.J. Stang (Eds.), Acetylene Chemistry: Chemistry, Biology and Materials Science, Wiley-VCH, Weinheim, 2004.
[6] F. Paul, C. Lapinte, Coord. Chem. Rev. 178–180 (1998) 431.
[7] C. Lapinte, J. Organomet. Chem. 693 (2008) 793.
[8] I.R. Whittall, A.M. McDonagh, M.G. Humphrey, M. Samoc, Adv. Organomet. Chem. 42 (1998) 291.
[9] W.-Y. Wong, C.-L. Ho, Coord. Chem. Rev. 250 (2006) 2627.
[10] W.-Y. Wong, X.-Z. Wang, Z. He, A.B. Djurii, C.-T. Yip, K.-Y. Cheung, H. Wang, C.S.K. Mak, W.-K. Chan, Nat. Mater. 6 (2007) 521.
[11] M.I. Bruce, P.J. Low, Adv. Organomet. Chem. 50 (2004) 179.
[12] N. LeNarvor, L. Toupet, C. Lapinte, J. Am. Chem. Soc. 117 (1995) 7129.
[13] R. Dembinski, T. Bartik, B. Bartik, M. Jaeger, J.A. Gladysz, J. Am. Chem. Soc. 122 (2000) 810.
[14] M. Brady, W.Q. Weng, Y.L. Zhou, J.W. Seyler, A.J. Amoroso, A.M. Arif, M. Bohme, G. Frenking, J.A. Gladysz, J. Am. Chem. Soc. 119 (1997) 775.
[15] Y.L. Zhou, J.W. Seyler, W.Q. Weng, A.M. Arif, J.A. Gladysz, J. Am. Chem. Soc. 115 (1993) 8509.
[16] M.I. Bruce, P.J. Low, K. Costuas, J.F. Halet, S.P. Best, G.A. Heath, J. Am. Chem. Soc. 122 (2000) 1949.
[17] S. Kheradmandan, K. Heinze, H.W. Schmalle, H. Berke, Angew. Chem. Int. Ed. 38 (1999) 2270.
[18] M. Mayor, C. von Hanisch, H.B. Weber, J. Reichert, D. Beckmann, Angew. Chem. Int. Ed. 41 (2002) 1183.
[19] K.-T. Wong, J.-M. Lehn, S.-M. Peng, G.-H. Lee, Chem. Commun. (2000) 2259.
[20] C. Olivier, B. Kim, D. Touchard, S. Rigaut, Organometallics 27 (2008) 509.
[21] B. Kim, J.M. Beebe, C. Olivier, S. Rigaut, D. Touchard, J.G. Kushmerick, X.-Y. Zhu, C.D. Frisbie, J. Phys. Chem. C 111 (2007) 7521.
[22] F.A. Cotton, R.A. Walton, Multiple Bonds Between Metal Atoms, Oxford Press, Oxford, 1993.
[23] T. Ren, Organometallics 24 (2005) 4854.
[24] J.L. Bear, B. Han, S. Huang, J. Am. Chem. Soc. 115 (1993) 1175.
[25] J.L. Bear, B. Han, S. Huang, K.M. Kadish, Inorg. Chem. 35 (1996) 3012.
[26] T. Ren, Organometallics 21 (2002) 732.
[27] G.L. Xu, T. Ren, Organometallics 20 (2001) 2400.
[28] G.L. Xu, T. Ren, J. Organomet. Chem. 655 (2002) 239.
[29] S.K. Hurst, T. Ren, J. Organomet. Chem. 660 (2002) 1.
[30] G. Zou, J.C. Alvarez, T. Ren, J. Organomet. Chem. 596 (2000) 152.

[31] G.L. Xu, C. Campana, T. Ren, Inorg. Chem. 41 (2002) 3521.
[32] C. Lin, T. Ren, E.J. Valente, J.D. Zubkowski, Dalton Trans. (1998) 571.
[33] C. Lin, T. Ren, E.J. Valente, J.D. Zubkowski, J. Organomet. Chem. 579 (1999) 114.
[34] G.L. Xu, T. Ren, Inorg. Chem. 40 (2001) 2925.
[35] T. Ren, G. Zou, J.C. Alvarez, Chem. Commun. (2000) 1197.
[36] G.L. Xu, G. Zou, Y.H. Ni, M.C. DeRosa, R.J. Crutchley, T. Ren, J. Am. Chem. Soc. 125 (2003) 10057.
[37] G.-L. Xu, A. Cordova, T. Ren, J. Cluster Sci. 15 (2004) 413.
[38] B. Xi, G.L. Xu, J.W. Ying, H.L. Han, A. Cordova, T. Ren, J. Organomet. Chem. 693 (2008) 1656.
[39] P. Siemsen, R.C. Livingston, F. Diederich, Angew. Chem. Int. Ed. 39 (2000) 2632.
[40] B. Bartik, R. Dembinski, T. Bartik, A.M. Arif, J.A. Gladysz, New J. Chem. 21 (1997) 739.
[41] C. Creutz, Prog. Inorg. Chem. 30 (1983) 1.
[42] D.E. Richardson, H. Taube, Inorg. Chem. 20 (1981) 1278.
[43] R.J. Crutchley, Adv. Inorg. Chem. 41 (1994) 273.
[44] J.P. Launay, Chem. Soc. Rev. 30 (2001) 386.
[45] G.L. Xu, C.Y. Wang, Y.H. Ni, T.G. Goodson, T. Ren, Organometallics 24 (2005) 3247.
[46] P.F. Barbara, T.J. Meyer, M.A. Ratner, J. Phys. Chem. 100 (1996) 13148.
[47] W.E. Geiger, Organometallics 26 (2007) 5738.
[48] P.J. Mosher, G.P.A. Yap, R.J. Crutchley, Inorg. Chem. 40 (2001) 1189.
[49] N.S. Hush, Prog. Inorg. Chem. 8 (1967) 391.
[50] M.B. Robin, P. Day, Adv. Inorg. Chem. Radiochem. 10 (1967) 247.
[51] B.S. Brunschwig, C. Creutz, N. Sutin, Chem. Soc. Rev. 31 (2002) 168.
[52] C.E.B. Evans, M.L. Naklicki, A.R. Rezvani, C.A. White, V.V. Kondratiev, R.J. Crutchley, J. Am. Chem. Soc. 120 (1998) 13096.
[53] A.C. Ribou, J.P. Launay, K. Takahashi, T. Nihira, S. Tarutani, C.W. Spangler, Inorg. Chem. 33 (1994) 1325.
[54] A.C. Ribou, J.P. Launay, M.L. Sachtleben, H. Li, C.W. Spangler, Inorg. Chem. 35 (1996) 3735.
[55] S.H. Choi, B. Kim, C.D. Frisbie, Science 320 (2008) 1482.
[56] M.Y. Ogawa, Mol. Supramol. Photochem. 4 (1999) 113.
[57] G.L. Xu, M.C. DeRosa, R.J. Crutchley, T. Ren, J. Am. Chem. Soc. 126 (2004) 3728.
[58] G.L. Xu, R.J. Crutchley, M.C. DeRosa, Q.J. Pan, H.X. Zhang, X.P. Wang, T. Ren, J. Am. Chem. Soc. 127 (2005) 13354.
[59] S. Barlow, D. Ohare, Chem. Rev. 97 (1997) 637.
[60] G.L. Xu, C.G. Jablonski, T. Ren, J. Organomet. Chem. 683 (2003) 388.
[61] S.K. Hurst, G.L. Xu, T. Ren, Organometallics 22 (2003) 4118.
[62] J.W. Ying, D.R. Sobransingh, G.L. Xu, A.E. Kaifer, T. Ren, Chem. Commun. (2005) 357.
[63] J.W. Ying, A. Cordova, T.Y. Ren, G.L. Xu, T. Ren, Chem. Eur. J. 13 (2007) 6874.
[64] R.D. Adams, B. Qu, M.D. Smith, Organometallics 21 (2002) 3867.
[65] C. Levanda, K. Bechgaard, D.O. Cowan, J. Org. Chem. 41 (1976) 2700.
[66] M.J. Powers, T.J. Meyer, J. Am. Chem. Soc. 100 (1978) 4393.
[67] Y.B. Zhu, O. Clot, M.O. Wolf, G.P.A. Yap, J. Am. Chem. Soc. 120 (1998) 1812.
[68] A.S. Blum, T. Ren, D.A. Parish, S.A. Trammell, M.H. Moore, J.G. Kushmerick, G.-L. Xu, J.R. Deschamps, S.K. Pollack, R. Shashidhar, J. Am. Chem. Soc. 127 (2005) 10010.
[69] A.K. Mahapatro, J. Ying, T. Ren, D.B. Janes, Nano Lett. 8 (2008) 2131.
[70] Q. Zheng, J.A. Gladysz, J. Am. Chem. Soc. 127 (2005) 10508.
[71] Q. Zheng, J.C. Bohling, T.B. Peters, A.C. Frisch, F. Hampel, J.A. Gladysz, Chem. Eur. J. 12 (2006) 6486.